Nonlinear Dyn
https://doi.org/10.1007/s11071-025-10972-0

RESEARCH

Exploration of soliton solutions and modulation instability analysis for cold bosonic atoms in a zig-zag optical lattice in quantum physics

Bahadır Kopçasız

Received: 16 December 2024 / Accepted: 4 February 2025

Abstract This paper investigates the widely used zig-zag optical lattice prototype for cold bosonic atoms. This prototype generally represents nonlinear waves in quantum physics. To investigate the soliton solutions of the offered equation, we consider two analytical solution methods. The first is a new version of the generalized exponential rational function method (nGERFM), and the second is the $\left(\frac{G'}{G^2}\right)$-expansion function method. The nGERFM facilitates the generation of multiple solution types, including singular, shock, singular periodic, exponential, combo trigonometric, and hyperbolic solutions in mixed forms. Thanks to the $\left(\frac{G'}{G^2}\right)$-expansion function method, we obtain trigonometric, hyperbolic, and rational solutions. The modulation instability of the offered prototype is discussed, with numerical simulations complementing the analytical outcomes to better understand the solutions' dynamic behavior. The findings are novel and can be useful for studying bosonic superfluidity, quantum magnetism, many-body spin dynamics, and Bose–Einstein condensation, among other studies involving ultracold atoms. These outcomes propose a foundation for future examination, making the solutions effective, manageable, and reliable for tackling complex nonlinear problems. The methodologies used in this study are robust, influential, and practicable for diverse nonlinear partial differential equations; to our knowledge, these methods of investigation have not been explored before for this equation.

Keywords Mathematical modelling · nGERFM · $\left(\frac{G'}{G^2}\right)$-expansion function method · Modulation instability (MI) · Soliton solutions

B. Kopçasız (✉)
Department of Computer Engineering, Faculty of Engineering and Architecture, Istanbul Gelisim University, Istanbul, Turkey
e-mail: bkopcasiz@gelisim.edu.tr

1 Introduction

The advancement of numerous scientific and engineering disciplines has been significantly facilitated by nonlinear partial differential equations (NLPDEs), which offer critical insights into the complexities of physical and biological processes. The historical evolution of NLPDEs can be traced back to the 18th and 19th centuries when mathematicians and physicists began formulating mathematical models to describe natural phenomena. Initially arising within the realms of fluid dynamics, heat transfer, and wave propagation, these equations have since been applied across a diverse range of fields, including electrical engineering, magnetism, quantum mechanics, and biological systems. Over time, the study and resolution of NLPDEs have progressed, propelled by both theoretical developments and the increasing capabilities of computational methods, resulting in enhanced understanding and more precise modeling of intricate systems [1–10].

In the 19th century, Scottish engineer John Scott Russell first identified solitons, remarkable nonlinear wave phenomena that maintain their shape while propagating at a constant speed. He observed a solitary wave that traveled significant distances without dissipating, which captivated scientists for many years. The mathematical framework for solitons was subsequently established in the 1960s by introducing the Korteweg-de Vries (KdV) equation, which characterizes shallow water waves. Since then, solitons have found applications in various fields, including fiber optic communications, where they facilitate stable, long-distance data transmission; plasma physics, where they elucidate phenomena in magnetic fields; and even biological systems, such as the propagation of nerve impulses. The study of solitons enhances our understanding of nonlinear wave dynamics and stimulates technological innovations across multiple domains [11–16].

Analytical solutions to NLPDEs offer significant insights into the behavior of complex systems governed by these equations. In contrast to their linear counterparts, NLPDEs often exhibit intricate and varied phenomena, such as shock waves, solitons, and turbulence rendering, their solutions highly valuable and challenging to obtain. Analytical methods seek to derive exact solutions or simplifications that illuminate the underlying structure and dynamics of the problem. Techniques such as the separation of variables, similarity transformations, the method of characteristics, and the inverse scattering transform has been developed to address specific classes of NLPDEs. These methodologies not only enhance our understanding of the fundamental properties of the solutions but also provide benchmarks for validating numerical and approximate solutions. Despite their inherent complexity, analytical solutions remain a cornerstone in the study of NLPDEs, contribute clarity and depth to the investigation of nonlinear systems across physics, engineering, and other disciplines. In the present day, there are numerous trustworthy and well-developed techniques for finding both analytic and numerical solutions to NLPDEs, including the well-regarded Lie group theory [17], the bilinear neural network method [18], ϕ^6-expansion technique [19], the new generalized exponential differential function approach [20], improved modified Sardar sub-equation method [21–23], extended Fan sub-equation method [24], extended hyperbolic function method [25], Sumudu transform homotopy perturbation method (STHPM) [26], q-homotopy analysis transform method [27], residual power series method (RPSM) [28], Kumar-Malik method [29,30], the improved generalized Riccati equation mapping method [31–33], the modified F-expansion method [34], the generalized Kudryashov method [35], Hirota's bilinear technique [36], the unified method [37,38], and so on.

Quantum physics has been increasingly important in recent years, with a significant growth trend continuing. The relevance of the theory of quantum fields to physics is illustrated by multiple frameworks. Investigating many body quantum states are made possible by the system of ultracold bosonic atoms in the optical lattice. By using a Bose–Hubbard model, this quantum lattice gas system is described [39]. The primary aim of this study is to create optical soliton patterns in a zig-zag optical lattice prototype for a cold bosonic atom [40,41]:

$$
\begin{aligned}
i\frac{d\Xi}{dt} &= (\alpha_1 - 2\alpha_2 - \alpha_3)\Xi - \tau^2(\alpha_2+\alpha_3)\frac{d^2\Xi}{dx^2} \\
&\quad +\alpha_4(y-1)\,|\Xi|^2\,\Xi,
\end{aligned}
\tag{1}
$$

where τ expresses the distance between successive components and the complex amplitude $\Xi = \Xi\,(x,t)$ is the wave function. The boson-boson interaction in the optical zig-zag lattice model is represented by the symbol α_4, which shows repulsion for $\alpha_4 > 0$ and attraction for $\alpha_4 < 0$. Whereas the second nearest-neighbor hopping requires $\alpha_2 > 0$, the first nearest-neighbor hopping involves $\alpha_1 > 0$. To study quantum phase transitions and other topics like Bose–Einstein condensation, quantum magnetism, many-body spin dynamics, and bosonic superfluidity, among others, experiments with ultracold atoms are essential.

The zig-zag optical lattice model considered in this study serves as a prototype for describing the behavior of cold bosonic atoms in ultracold systems. This model is particularly significant in quantum physics, as it captures the intricate dynamics of nonlinear wave propagation in structured optical lattices. The zig-zag configuration introduces additional complexity by incorporating geometric and topological features, making it a valuable framework for studying phenomena such as bosonic superfluidity, quantum magnetism, many-body spin dynamics, and Bose–Einstein condensation. The NLPDE governing this model reflects the interplay between nonlinearity and dispersion, which is crucial for the formation of solitons and understanding modulation instability. By addressing this model, the study provides a comprehensive exploration of its soliton solutions and dynamic properties, offering new insights into the behavior of nonlinear waves in complex quantum systems.

To determine the soliton solutions for the model under investigation, numerous researchers have employed a range of techniques. Riaz et al. obtained solutions for the studied equation using the generalized logistic equation method and the Sardar subequation approach [40]. They also analyzed the bifurcation theory and the chaotic behavior. Using two efficient methods, S. Kumar and A. Kumar developed for Eq. (1) a variety of soliton patterns [42]. By using semi-inverse techniques and collective variables to assess the investigated model, Alhussain and Raza achieved their goal of identifying brilliant solitons [43].

The principal aim of this study is to investigate different and novel optical soliton solutions for Eq. (1). In this sense, nGERFM and the $\left(\frac{G'}{G^2}\right)$-expansion function method are used. The most significant findings of this study include the discovery of novel classes of soliton solutions for the zig-zag optical lattice prototype, which had not been presented before. Using the nGERFM, we derived a diverse range of solutions, including singular, shock, singular periodic, exponential, combo trigonometric, and hyperbolic solutions in mixed forms. Additionally, by employing the $\left(\frac{G'}{G^2}\right)$-expansion function method, trigonometric, hyperbolic, and rational solutions were obtained. These findings go beyond existing studies by providing an exhaustive range of soliton structures, allowing for a deeper understanding of the dynamic behavior of nonlinear waves in quantum systems. The outcomes are particularly significant because they offer validated solutions applicable to various NLPDEs and contribute to advancing the study of cold bosonic atoms, quantum magnetism, many-body spin dynamics, and Bose–Einstein condensation in ultracold systems.

The applied methods in this study offer significant advantages over existing techniques in the literature. The nGERFM facilitates the generation of a broad spectrum of solution types, including singular, shock, singular periodic, exponential, combo trigonometric, and hyperbolic solutions, often in mixed forms, while the $\left(\frac{G'}{G^2}\right)$-expansion function method yields trigonometric, hyperbolic, and rational solutions. This diversity surpasses many conventional methods, which are often limited to a narrower range of solution types. Additionally, these methods follow a systematic and structured approach, making them effective for identifying and organizing solution structures from the outset. Their flexibility and reliability in solving NLPDEs make them highly applicable across various fields, including quantum physics, nonlinear dynamics, and applied sciences. However, one limitation of these methods is that they may not work as effectively when the largest derivative and the nonlinear terms in the equation are not balanced or homogeneous. In such cases, the methods may fail to produce valid solutions, highlighting the importance of ensuring proper balancing within the equation for successful application.

The following is the structure of the paper: The nGERFM and the $\left(\frac{G'}{G^2}\right)$-expansion function methods are explained in Sect. 2. In Sect. 3, the model's analytical solutions are obtained. In Sect. 4, the modulation instability analysis is presented. In Sect. 5, graphical explanations are provided. Comparisons are offered in Sect. 6, and conclusions are discussed in Sect. 7.

2 Analysis of the offered techniques

In this part, we explore two analytical techniques: the nGERFM and the $\left(\frac{G'}{G^2}\right)$-expansion function method. A wide description of the presented techniques is supplied within this part.

Let us consider the following NLPDE

$$Q_1(\Xi, \Xi_t, \Xi_x, \Xi_{xx}, \ldots) = 0. \tag{2}$$

To get traveling wave solutions for the concerned prototype, we employ the subsequent transformation:

$$\Xi = \Phi(\xi) \times \exp(i(\gamma x + \theta t + \delta), \xi = sx - \eta t, \tag{3}$$

where η is the wave velocity and s is the wave number.

Eq. (2) is altered into an ODE as shown:

$$Q_2(\Phi, \Phi', \Phi'', \Phi''', \ldots) = 0. \tag{4}$$

2.1 Description of the nGERFM

Step 1. Let we set up the solution of Eq. (4) as [44]:

$$\Phi(\xi) = k_0 + \sum_{n=1}^{n_0} k_n \left(\frac{\daleth'(\xi)}{\daleth(\xi)}\right)^n + \sum_{n=1}^{n_0} l_n \left(\frac{\daleth'(\xi)}{\daleth(\xi)}\right)^{-n}, \tag{5}$$

in which

$$\daleth(\xi) = \frac{\varsigma_1 \exp(\jmath_1\xi) + \varsigma_2 \exp(\jmath_2\xi)}{\varsigma_3 \exp(\jmath_3\xi) + \varsigma_4 \exp(\jmath_4\xi)}. \tag{6}$$

In the pre-assumed structures Eqs. (6) and (5), ς_i, $\jmath_i$ ($i \in [1, 4]$) and k_0, k_n, l_n ($n \in [1, n_0]$) are unknown coefficients. In addition, to determine the value of the positive integer n_0, we can make use of various balancing rules documented in the literature.

Step 2. Substituting the expression from Eq. (5) into Eq. (4) produces a polynomial equation $\Pi(\varrho_1, \varrho_2, \varrho_3, \varrho_4) = 0$ in terms of $\varrho_n = e^{(\jmath_v \xi)}$ for $v = 1, 2, 3, 4$.

Step 3. At last, we obtain analytical solutions for Eq. (2) by substituting the results derived from solving this system into the general expression of Eq. (5).

2.2 The summary of $\left(\frac{G'}{G^2}\right)$-expansion function method

Step 1. Suppose the solution of Eq. (4) is characterized by the expression in $\left(\frac{G'}{G^2}\right)$-expansion method as follows [44]:

$$\Phi(\xi) = \rho_0 + \sum_{n=1}^{n_0} \left(\rho_n \left(\frac{G'}{G^2}\right)^n + \sigma_n \left(\frac{G'}{G^2}\right)^{-n} \right), \tag{7}$$

in which $G = G(\xi)$ holds

$$\left(\frac{G'}{G^2}\right)' = \mu + \lambda \left(\frac{G'}{G^2}\right)^2, \tag{8}$$

where $\lambda \neq 0$, $\mu \neq 1$ are integers. To complete the process, it is necessary to find the constants ρ_0, ρ_n, σ_n ($n = 1, 2, 3, \ldots, n_0$).

Step 2. As a result, $\left(\frac{G'}{G^2}\right)$ provides the following three types of solutions:

Scenario I, Trigonometric family: If $\mu\lambda > 0$, then

$$\left(\frac{G'}{G^2}\right) = \sqrt{\frac{\mu}{\lambda}} \left(\frac{\Theta_1 \cos\left(\sqrt{\mu\lambda}\xi\right) + \Theta_2 \sin\left(\sqrt{\mu\lambda}\xi\right)}{\Theta_2 \cos\left(\sqrt{\mu\lambda}\xi\right) - \Theta_1 \sin\left(\sqrt{\mu\lambda}\xi\right)} \right). \tag{9}$$

Scenario II, Hyperbolic family: When $\mu\lambda < 0$, then

$$\left(\frac{G'}{G^2}\right) = -\frac{\sqrt{|\mu\lambda|}}{\lambda} \left(\frac{\Theta_1 \sinh\left(2\sqrt{|\mu\lambda|}\xi\right) + \Theta_1 \cosh\left(2\sqrt{|\mu\lambda|}\xi\right) + \Theta_2}{\Theta_1 \sinh\left(2\sqrt{|\mu\lambda|}\xi\right) + \Theta_1 \cosh\left(2\sqrt{|\mu\lambda|}\xi\right) - \Theta_2} \right). \tag{10}$$

Scenario III, Rational family: When $\mu = 0$, $\lambda \neq 0$, then

$$\left(\frac{G'}{G^2}\right) = \left(-\frac{\Theta_1}{\lambda\left(\Theta_1 \xi + \Theta_2\right)} \right), \tag{11}$$

in which Θ_1 and Θ_2 are constants.

Step 3. To find the n_0, the homogeneous balance rule is applied.

Step 4. By inserting from Eq. (7) and Eq. (8) into Eq. (3), we get a set of algebraic equations.

Step 5. By investigating the specific terms, we found the necessary set of parameter.

3 Extraction of soliton solutions

This part covers the soliton solutions and their visual representations in association with the prototype under study. By inserting Eq. (3) into Eq. (1), we derive the following nonlinear equation.

Real part:

$$\left[\gamma^2 \tau^2 (\alpha_2 + 4\alpha_3) + \theta + \alpha_1 - 2(\alpha_2 + \alpha_3)\right] \Phi + \alpha_4 (y - 1)\Phi^3 - s^2 \tau^2 (\alpha_2 + 4\alpha_3)\Phi'' = 0, \tag{12}$$

and imaginary part:

$$\left[-\eta + 2\gamma s \tau^2 (\alpha_2 + 4\alpha_3)\right] = 0. \tag{13}$$

From Eq. (13), the velocity can be expressed as,

$$\eta = 2\gamma s \tau^2 (\alpha_2 + 4\alpha_3). \tag{14}$$

$3n_0 = n_0 + 2$ is obtained by using certain standard balancing principles in Eq. (12) between Φ^3 and Φ''. Hence, one should take $n_0 = 1$.

3.1 Main results of solving model Eq. (1) using the nGERFM

Eq. (5) can be expressed as

$$\Phi(\xi) = k_0 + k_1 \left(\frac{\daleth'(\xi)}{\daleth(\xi)}\right) + l_1 \left(\frac{\daleth'(\xi)}{\daleth(\xi)}\right)^{-1}. \tag{15}$$

$\urcorner(\xi)$ is specified by Eq. (6).

Class 1:

Taking $[\varsigma_1, \varsigma_2, \varsigma_3, \varsigma_4] = [1, 1, 1, 0]$ and $[\jmath_1, \jmath_2, \jmath_3, \jmath_4] = [0, 1, 2, 0]$ in Eq. (6) yields

$$\urcorner(\xi) = \frac{1+\exp(\xi)}{\exp(2\xi)}. \tag{16}$$

To obtain the parameter values, we solve the algebraic equations with Maple (or Mathematica). The collection of responses generated might be given as:

Type 1.1:

$$\begin{aligned}\theta &= -\gamma^2\tau^2\alpha_2 - 4\gamma^2\tau^2\alpha_3 \\ &\quad -\frac{1}{2}s^2\tau^2\alpha_2 - 2s^2\tau^2\alpha_3 - \alpha_1 + 2\alpha_2 + 2\alpha_3, \\ k_0 &= \mp\frac{\tau s 5\sqrt{2}}{2}\sqrt{\frac{\alpha_2+4\alpha_3}{\alpha_4(y-1)}}, k_1 \\ &\quad = \pm\tau s\sqrt{2}\sqrt{\frac{\alpha_2+4\alpha_3}{\alpha_4(y-1)}}, l_1 = 0.\end{aligned}$$

By plugging the aforementioned values of k_0, k_1, l_1 into Eq. (15), we get

$$\Phi^{\pm}(\xi) = \frac{\tau s\sqrt{2}}{2}\sqrt{\frac{\alpha_2+4\alpha_3}{\alpha_4(y-1)}} \times \left(\frac{\exp(\xi)-1}{\exp(\xi)+1}\right). \tag{17}$$

We find the following exponential function solution for Eq. (1) using Eq. (17)

$$\begin{aligned}\Xi^{\pm}_{1,1}(x,t) &= \frac{\tau s\sqrt{2}}{2}\sqrt{\frac{\alpha x_2+4\alpha_3}{\alpha_4(y-1)}} \\ &\times \left(\frac{\exp(sx - \left(2\gamma s\tau^2(\alpha_2+4\alpha_3)\right)t) - 1}{\exp(sx - \left(2\gamma s\tau^2(\alpha_2+4\alpha_3)\right)t) + 1}\right) \\ &\times \exp\left(i\left(\gamma x + \begin{pmatrix} -\gamma^2\tau^2\alpha_2 - 4\gamma^2\tau^2\alpha_3 \\ -\frac{1}{2}s^2\tau^2\alpha_2 - 2s^2\tau^2\alpha_3 \\ -\alpha_1 + 2\alpha_2 + 2\alpha_3 \end{pmatrix} t + \delta\right)\right).\end{aligned} \tag{18}$$

Type 1.2:

$$\begin{aligned}\theta &= -\gamma^2\tau^2\alpha_2 - 4\gamma^2\tau^2\alpha_3 - \frac{1}{2}s^2\tau^2\alpha_2 \\ &-2s^2\tau^2\alpha_3 - \alpha_1 + 2\alpha_2 + 2\alpha_3, \\ k_0 &= \mp\frac{\tau s 5\sqrt{2}}{2}\sqrt{\frac{\alpha_2+4\alpha_3}{\alpha_4(y-1)}}, k_1 \\ &= 0, l_1 = \pm\tau s 6\sqrt{2}\sqrt{\frac{\alpha_2+4\alpha_3}{\alpha_4(y-1)}}.\end{aligned}$$

By substituting the aforementioned values of k_0, k_1, l_1 into Eq. (15), we get

$$\begin{aligned}\Phi^{\mp}(\xi) &= \frac{\tau s\sqrt{2}}{2}\sqrt{\frac{\alpha_2+4\alpha_3}{\alpha_4(y-1)}} \\ &\times \left(\frac{3\exp(\xi)-2}{3\exp(\xi)+2}\right).\end{aligned} \tag{19}$$

The exponential function solution for Eq. (1) is found using Eq. (19) in the following manner:

$$\begin{aligned}\Xi^{\mp}_{1,2}(x,t) &= \frac{\tau s\sqrt{2}}{2}\sqrt{\frac{\alpha_2+4\alpha_3}{\alpha_4(y-1)}} \\ &\times \left(\frac{3\exp(sx - \left(2\gamma s\tau^2(\alpha_2+4\alpha_3)\right)t) - 2}{3\exp(sx - \left(2\gamma s\tau^2(\alpha_2+4\alpha_3)\right)t) + 2}\right) \\ &\times \exp\left(i\left(\gamma x + \begin{pmatrix} -\gamma^2\tau^2\alpha_2 - 4\gamma^2\tau^2\alpha_3 \\ -\frac{1}{2}s^2\tau^2\alpha_2 - 2s^2\tau^2\alpha_3 \\ -\alpha_1 + 2\alpha_2 + 2\alpha_3 \end{pmatrix} t + \delta\right)\right).\end{aligned} \tag{20}$$

Class 2:

When we pick $[\varsigma_1, \varsigma_2, \varsigma_3, \varsigma_4] = [1, -1, 2i, 0]$ and $[\jmath_1, \jmath_2, \jmath_3, \jmath_4] = [i, -i, 1, 0]$ in Eq. (6), we reach

$$\urcorner(\xi) = \frac{\sin(\xi)}{\exp(\xi)}. \tag{21}$$

To acquire parameter values, we use package programs to solve algebraic equations; the collection of solutions that result can be stated as:

Type 2.1:

$$\begin{aligned}&\theta = -\gamma^2\tau^2\alpha_2 - 4\gamma^2\tau^2\alpha_3 + 2s^2\tau^2\alpha_2 \\ &+8s^2\tau^2\alpha_3 - \alpha_1 + 2\alpha_2 + 2\alpha_3, \\ &k_0 = \pm\frac{\sqrt{2}\tau s\,(\alpha_2+4\alpha_3)}{\alpha_4(y-1)\sqrt{\frac{\alpha_2+4\alpha_3}{\alpha_4(y-1)}}}, k_1 \\ &= \pm\tau s\sqrt{2}\sqrt{\frac{\alpha_2+4\alpha_3}{\alpha_4(y-1)}}, l_1 = 0.\end{aligned}$$

These values are entered into Eq. (15), yielding

$$\Phi^{\pm}(\xi) = \tau s\sqrt{2}\sqrt{\frac{\alpha_2 + 4\alpha_3}{\alpha_4(y-1)}} \times \cot(\xi). \tag{22}$$

By employing Eq. (22), we derive the singular periodic solution for Eq. (1) as follows:

$$\Xi^{\pm}_{2,1}(x,t) = \tau s\sqrt{2}\sqrt{\frac{\alpha_2 + 4\alpha_3}{\alpha_4(y-1)}} \times \cot\left(sx - \left(2\gamma s\tau^2(\alpha_2 + 4\alpha_3)\right)t\right) \times \exp\left(i\left(\gamma x + \begin{pmatrix} -\gamma^2\tau^2\alpha_2 - 4\gamma^2\tau^2\alpha_3 \\ +2s^2\tau^2\alpha_2 + 8s^2\tau^2\alpha_3 \\ -\alpha_1 + 2\alpha_2 + 2\alpha_3 \end{pmatrix} t + \delta\right)\right). \tag{23}$$

Type 2.2:

$$\theta = -\gamma^2\tau^2\alpha_2 - 4\gamma^2\tau^2\alpha_3 + 2s^2\tau^2\alpha_2 + 8s^2\tau^2\alpha_3 - \alpha_1 + 2\alpha_2 + 2\alpha_3,$$

$$k_0 = \pm\tau s\sqrt{2}\sqrt{\frac{\alpha_2 + 4\alpha_3}{\alpha_4(y-1)}}, k_1 = 0, l_1 = \pm 2\sqrt{2}\tau s\sqrt{\frac{\alpha_2 + 4\alpha_3}{\alpha_4(y-1)}}.$$

These values are entered into Eq. (15), yielding

$$\Phi^{\pm}(\xi) = \tau s\sqrt{2}\sqrt{\frac{\alpha_2 + 4\alpha_3}{\alpha_4(y-1)}} \times \left(\frac{\cos(\xi) + \sin(\xi)}{\cos(\xi) - \sin(\xi)}\right). \tag{24}$$

By substituting Eq. (24), we derive the following combo trigonometric solution for Eq. (1):

$$\Xi^{\pm}_{2,2}(x,t) = \tau s\sqrt{2}\sqrt{\frac{\alpha_2 + 4\alpha_3}{\alpha_4(y-1)}} \times \left(\frac{\cos\left(sx - \left(2\gamma s\tau^2(\alpha_2 + 4\alpha_3)\right)t\right) + \sin\left(sx - \left(2\gamma s\tau^2(\alpha_2 + 4\alpha_3)\right)t\right)}{\cos\left(sx - \left(2\gamma s\tau^2(\alpha_2 + 4\alpha_3)\right)t\right) - \sin\left(sx - \left(2\gamma s\tau^2(\alpha_2 + 4\alpha_3)\right)t\right)}\right) \times \exp\left(i\left(\gamma x + \begin{pmatrix} -\gamma^2\tau^2\alpha_2 - 4\gamma^2\tau^2\alpha_3 \\ +2s^2\tau^2\alpha_2 + 8s^2\tau^2\alpha_3 \\ -\alpha_1 + 2\alpha_2 + 2\alpha_3 \end{pmatrix} t + \delta\right)\right). \tag{25}$$

Class 3:

For $[\varsigma_1, \varsigma_2, \varsigma_3, \varsigma_4] = [1, -1, 2, 0]$ and $[\jmath_1, \jmath_2, \jmath_3, \jmath_4] = [1, -1, -1, 0]$ in Eq. (6) provides

$$\daleth(\xi) = \frac{\sinh(\xi)}{\exp(-\xi)}. \tag{26}$$

By implementing **the nGERFM** procedure, we obtain

$$\theta = -\gamma^2\tau^2\alpha_2 - 4\gamma^2\tau^2\alpha_3 - 2s^2\tau^2\alpha_2 - 8s^2\tau^2\alpha_3 - \alpha_1 + 2\alpha_2 + 2\alpha_3,$$

$$k_0 = \pm\frac{\sqrt{2}\tau s\,(\alpha_2 + 4\alpha_3)}{\alpha_4(y-1)\sqrt{\frac{\alpha_2+4\alpha_3}{\alpha_4(y-1)}}},$$

$$k_1 = \pm\tau s\sqrt{2}\sqrt{\frac{\alpha_2 + 4\alpha_3}{\alpha_4(y-1)}}, l_1 = 0.$$

These values are entered into Eq. (15), yielding

$$\Phi^{\mp}(\xi) = \frac{\sqrt{2}\tau s\,(\alpha_2 + 4\alpha_3)}{\alpha_4(y-1)\sqrt{\frac{\alpha_2+4\alpha_3}{\alpha_4(y-1)}}} \times \tanh(\xi). \tag{27}$$

By using Eq. (27), we reach the next shock solution for Eq. (1)

$$\Xi^{\mp}_{3}(x,t) = \frac{\sqrt{2}\tau s\,(\alpha_2 + 4\alpha_3)}{\alpha_4(y-1)\sqrt{\frac{\alpha_2+4\alpha_3}{\alpha_4(y-1)}}} \times \tanh\left(sx - \left(2\gamma s\tau^2(\alpha_2 + 4\alpha_3)\right)t\right) \times \exp\left(i\left(\gamma x + \begin{pmatrix} -\gamma^2\tau^2\alpha_2 - 4\gamma^2\tau^2\alpha_3 \\ -2s^2\tau^2\alpha_2 - 8s^2\tau^2\alpha_3 \\ -\alpha_1 + 2\alpha_2 + 2\alpha_3 \end{pmatrix} t + \delta\right)\right). \tag{28}$$

Class 4:

In Eq. (6), picking $[\varsigma_1, \varsigma_2, \varsigma_3, \varsigma_4] = [2, 0, 1, 1]$ and $[\jmath_1, \jmath_2, \jmath_3, \jmath_4] = [1, 0, i, -i]$ produces

$$\daleth(\xi) = \frac{\exp(\xi)}{\cos(\xi)}. \tag{29}$$

We also achieve

Type 4.1:

$$\theta = -\gamma^2\tau^2\alpha_2 - 4\gamma^2\tau^2\alpha_3 + 2s^2\tau^2\alpha_2 + 8s^2\tau^2\alpha_3 - \alpha_1 + 2\alpha_2 + 2\alpha_3,$$
$$k_0 = \pm\sqrt{2}\tau s\sqrt{\frac{\alpha_2+4\alpha_3}{\alpha_4(y-1)}}, k_1 = 0, l_1 = \mp 2\sqrt{2}\tau s\sqrt{\frac{\alpha_2+4\alpha_3}{\alpha_4(y-1)}}.$$

These findings combined with Eq. (15) produce

$$\Phi^{\pm}(\xi) = \sqrt{2}\tau s\sqrt{\frac{\alpha_2+4\alpha_3}{\alpha_4(y-1)}} \times \left(\frac{2\cos(\xi)\sin(\xi)-1}{2\cos(\xi)^2-1}\right). \quad (30)$$

As a result of our findings, the following combo trigonometric solution is achieved:

$$\Xi^{\pm}_{4,1}(x,t) = \sqrt{2}\tau s\sqrt{\frac{\alpha_2+4\alpha_3}{\alpha_4(y-1)}} \times \left(\frac{2\cos(sx-\eta t)\sin\left(sx-\left(2\gamma s\tau^2(\alpha_2+4\alpha_3)\right)t\right)-1}{2\cos\left(sx-\left(2\gamma s\tau^2(\alpha_2+4\alpha_3)\right)t\right)^2-1}\right) \times \exp\left(i\left(\gamma x + \begin{pmatrix} -\gamma^2\tau^2\alpha_2 - 4\gamma^2\tau^2\alpha_3 \\ +2s^2\tau^2\alpha_2 + 8s^2\tau^2\alpha_3 \\ -\alpha_1 + 2\alpha_2 + 2\alpha_3 \end{pmatrix} t + \delta\right)\right). \quad (31)$$

Type 4.2:

$$\theta = -\gamma^2\tau^2\alpha_2 - 4\gamma^2\tau^2\alpha_3 + 2s^2\tau^2\alpha_2 + 8s^2\tau^2\alpha_3 - \alpha_1 + 2\alpha_2 + 2\alpha_3,$$
$$k_0 = \mp\frac{\sqrt{2}\tau s(\alpha_2+4\alpha_3)}{\alpha_4(y-1)\sqrt{\frac{\alpha_2+4\alpha_3}{\alpha_4(y-1)}}}, k_1 = \pm\tau s\sqrt{2}\sqrt{\frac{\alpha_2+4\alpha_3}{\alpha_4(y-1)}}, \ l_1 = 0.$$

These findings combined with Eq. (15) yields

$$\Phi^{\pm}(\xi) = \frac{\sqrt{2}\tau s(\alpha_2+4\alpha_3)}{\alpha_4(y-1)\sqrt{\frac{\alpha_2+4\alpha_3}{\alpha_4(y-1)}}} \times \tan(\xi). \quad (32)$$

Therefore, one way to describe the singular periodic solution is as

$$\Xi^{\pm}_{4,2}(x,t) = \frac{\sqrt{2}\tau s(\alpha_2+4\alpha_3)}{\alpha_4(y-1)\sqrt{\frac{\alpha_2+4\alpha_3}{\alpha_4(y-1)}}} \times \tan\left(sx - \left(2\gamma s\tau^2(\alpha_2+4\alpha_3)\right)t\right) \times \exp\left(i\left(\gamma x + \begin{pmatrix} -\gamma^2\tau^2\alpha_2 - 4\gamma^2\tau^2\alpha_3 \\ +2s^2\tau^2\alpha_2 + 8s^2\tau^2\alpha_3 \\ -\alpha_1 + 2\alpha_2 + 2\alpha_3 \end{pmatrix} t + \delta\right)\right). \quad (33)$$

Class 5:

In Eq. (6), considering $[\varsigma_1, \varsigma_2, \varsigma_3, \varsigma_4] = [2, 0, 1, 1]$ and $[\jmath_1, \jmath_2, \jmath_3, \jmath_4] = [0, 0, 1, -1]$ generates

$$\daleth(\xi) = \frac{1}{\cosh(\xi)}. \quad (34)$$

We accomplish

Type 5.1:

$$\theta = -\gamma^2\tau^2\alpha_2 - 4\gamma^2\tau^2\alpha_3 - 2s^2\tau^2\alpha_2 - 8s^2\tau^2\alpha_3 - \alpha_1 + 2\alpha_2 + 2\alpha_3,$$
$$k_0 = 0, k_1 = \pm\tau s\sqrt{2}\sqrt{\frac{\alpha_2+4\alpha_3}{\alpha_4(y-1)}}, l_1 = 0.$$

By plugging the values of k_0, k_1, l_1 into Eq. (15), we gain

$$\Phi^{\mp}(\xi) = \tau s\sqrt{2}\sqrt{\frac{\alpha_2+4\alpha_3}{\alpha_4(y-1)}} \times \tanh(\xi). \quad (35)$$

As a result, we can derive shock soliton solution given by:

$$\Xi^{\mp}_{5,1}(x,t) = \tau s\sqrt{2}\sqrt{\frac{\alpha_2+4\alpha_3}{\alpha_4(y-1)}} \times \tanh\left(sx - \left(2\gamma s\tau^2(\alpha_2+4\alpha_3)\right)t\right) \times \exp\left(i\left(\gamma x + \begin{pmatrix} -\gamma^2\tau^2\alpha_2 - 4\gamma^2\tau^2\alpha_3 \\ -2s^2\tau^2\alpha_2 - 8s^2\tau^2\alpha_3 \\ -\alpha_1 + 2\alpha_2 + 2\alpha_3 \end{pmatrix} t + \delta\right)\right). \quad (36)$$

Type 5.2:

$$\theta = -\gamma^2\tau^2\alpha_2 - 4\gamma^2\tau^2\alpha_3 - 2s^2\tau^2\alpha_2 - 8s^2\tau^2\alpha_3 - \alpha_1 + 2\alpha_2 + 2\alpha_3,$$
$$k_0 = k_1 = 0, l_1$$

$$= \pm\tau s\sqrt{2}\sqrt{\frac{\alpha_2+4\alpha_3}{\alpha_4(y-1)}}.$$

By inserting the values of k_0, k_1, l_1 into Eq. (15), we gain

$$\Phi^{\mp}(\xi) = \tau s\sqrt{2}\sqrt{\frac{\alpha_2+4\alpha_3}{\alpha_4(y-1)}} \times \coth(\xi). \qquad (37)$$

As a result, we can derive singular soliton solution given by:

$$\Xi^{\mp}_{5,2}(x,t) = \tau s\sqrt{2}\sqrt{\frac{\alpha_2+4\alpha_3}{\alpha_4(y-1)}} \times \coth\left(sx - \left(2\gamma s\tau^2(\alpha_2+4\alpha_3)\right)t\right) \times \exp\left(i\left(\gamma x + \begin{pmatrix} -\gamma^2\tau^2\alpha_2 - 4\gamma^2\tau^2\alpha_3 \\ -2s^2\tau^2\alpha_2 - 8s^2\tau^2\alpha_3 \\ -\alpha_1 + 2\alpha_2 + 2\alpha_3 \end{pmatrix} t + \delta\right)\right). \qquad (38)$$

Type 5.3:

$$\theta = -\gamma^2\tau^2\alpha_2 - 4\gamma^2\tau^2\alpha_3 - 8s^2\tau^2\alpha_2 - 32s^2\tau^2\alpha_3 - \alpha_1 + 2\alpha_2 + 2\alpha_3,$$
$$k_0 = 0, k_1 = l_1 = \pm\tau s\sqrt{2}\sqrt{\frac{\alpha_2+4\alpha_3}{\alpha_4(y-1)}}.$$

For these reasons, along with Eq. (15), the following result is most likely to be achieved

$$\Phi^{\mp}(\xi) = \tau s\sqrt{2}\sqrt{\frac{\alpha_2+4\alpha_3}{\alpha_4(y-1)}} \times \left(\frac{2\cosh(\xi)^2 - 1}{\cosh(\xi)\sinh(\xi)}\right). \qquad (39)$$

The mixed form of the hyperbolic solution is expressed as

$$\Xi^{\mp}_{5,3}(x,t) = \tau s\sqrt{2}\sqrt{\frac{\alpha_2+4\alpha_3}{\alpha_4(y-1)}}\left(\frac{-1+2\cosh\left(sx-\left(2\gamma s\tau^2(\alpha_2+4\alpha_3)\right)t\right)^2}{\sinh(sx-\left(2\gamma s\tau^2(\alpha_2+4\alpha_3)\right)t)\cosh\left(sx-\left(2\gamma s\tau^2(\alpha_2+4\alpha_3)\right)t\right)}\right) \times \exp\left(i\left(\gamma x + \begin{pmatrix} -\gamma^2\tau^2\alpha_2 - 4\gamma^2\tau^2\alpha_3 \\ -8s^2\tau^2\alpha_2 - 32s^2\tau^2\alpha_3 \\ -\alpha_1 + 2\alpha_2 + 2\alpha_3 \end{pmatrix} t + \delta\right)\right). \qquad (40)$$

We reach

$$\theta = -\gamma^2\tau^2\alpha_2 - 4\gamma^2\tau^2\alpha_3 - 2s^2\tau^2\alpha_2 - 8s^2\tau^2\alpha_3 - \alpha_1 + 2\alpha_2 + 2\alpha_3,$$
$$k_0 = \pm 2\sqrt{2}\tau s\sqrt{\frac{\alpha_2+4\alpha_3}{\alpha_4(y-1)}}, k_1 = 0, l_1 = \pm 3\sqrt{2}\tau s\sqrt{\frac{\alpha_2+4\alpha_3}{\alpha_4(y-1)}}.$$

By entering the values of k_0, k_1, l_1 into Eq. (15), one gets

$$\Phi^{\pm}(\xi) = \sqrt{2}\tau s\sqrt{\frac{\alpha_2+4\alpha_3}{\alpha_4(y-1)}} \times \left(\frac{\cosh(\xi) + 2\sinh(\xi)}{\sinh(\xi) + 2\cosh(\xi)}\right). \qquad (42)$$

We arrive at the combo soliton solution by using the Eq. (42)

$$\Xi^{\pm}_{6}(x,t) = \sqrt{2}\tau s\sqrt{\frac{\alpha_2+4\alpha_3}{\alpha_4(y-1)}} \times \left(\frac{2\sinh(sx-\left(2\gamma s\tau^2(\alpha_2+4\alpha_3)\right)t) + \cosh(sx-\left(2\gamma s\tau^2(\alpha_2+4\alpha_3)\right)t)}{2\cosh(sx-\left(2\gamma s\tau^2(\alpha_2+4\alpha_3)\right)t) + \sinh(sx-\left(2\gamma s\tau^2(\alpha_2+4\alpha_3)\right)t)}\right) \times \exp\left(i\left(\gamma x + \begin{pmatrix} -\gamma^2\tau^2\alpha_2 - 4\gamma^2\tau^2\alpha_3 \\ -2s^2\tau^2\alpha_2 - 8s^2\tau^2\alpha_3 \\ -\alpha_1 + 2\alpha_2 + 2\alpha_3 \end{pmatrix} t + \delta\right)\right). \qquad (43)$$

Class 6:

In Eq. (6), considering $[\varsigma_1, \varsigma_2, \varsigma_3, \varsigma_4] = [2, 0, 1, 1]$ and $[\jmath_1, \jmath_2, \jmath_3, \jmath_4] = [-2, 0, 1, -1]$ generates

$$\daleth(\xi) = \frac{\exp(-2\xi)}{\cosh(\xi)}. \qquad (41)$$

Class 7:

If we take $[\varsigma_1, \varsigma_2, \varsigma_3, \varsigma_4] = [1, 1, 2, 0]$ and $[\jmath_1, \jmath_2, \jmath_3, \jmath_4] = [i, -i, 0, 0]$ in Eq. (6) provides

$$\daleth(\xi) = \cos(\xi). \qquad (44)$$

We have,

$$\theta = -\gamma^2\tau^2\alpha_2 - 4\gamma^2\tau^2\alpha_3 - 4s^2\tau^2\alpha_2 - 16s^2\tau^2\alpha_3 - \alpha_1 + 2\alpha_2 + 2\alpha_3,$$

$$k_0 = 0, k_1 = l_1 = \pm\tau s\sqrt{2}\sqrt{\frac{\alpha_2 + 4\alpha_3}{\alpha_4(y-1)}}.$$

When these results are analyzed in conjunction with Eq. (15), we get the following outcome

$$\Phi^{\mp}(\xi) = \tau s\sqrt{2}\sqrt{\frac{\alpha_2 + 4\alpha_3}{\alpha_4(y-1)}} \times \frac{1}{\cos(\xi)\sin(\xi)}. \tag{45}$$

As a result, we have the periodic solution given below:

$$\Xi_7^{\mp}(x,t) = \tau s\sqrt{2}\sqrt{\frac{\alpha_2 + 4\alpha_3}{\alpha_4(y-1)}} \times \frac{1}{\cos\left(sx - \left(2\gamma s\tau^2(\alpha_2+4\alpha_3)\right)t\right)\sin\left(sx - \left(2\gamma s\tau^2(\alpha_2+4\alpha_3)\right)t\right)} \times \exp\left(i\left(\gamma x + \begin{pmatrix} -\gamma^2\tau^2\alpha_2 - 4\gamma^2\tau^2\alpha_3 \\ -4s^2\tau^2\alpha_2 - 16s^2\tau^2\alpha_3 \\ -\alpha_1 + 2\alpha_2 + 2\alpha_3 \end{pmatrix} t + \delta\right)\right). \tag{46}$$

3.2 Main results of solving model Eq. (1) using the $\left(\frac{G'}{G^2}\right)$-expansion function method

Eq. (7) can be expressed as

$$\Phi(\xi) = \rho_0 + \rho_1\left(\frac{G'}{G^2}\right) + \sigma_1\left(\frac{G'}{G^2}\right)^{-1}, \tag{47}$$

in which ρ_0, ρ_1, and σ_1 are real parameters and are determined later. The use of Eqs. (12) and (47) together with Eq. (8) gives the cluster of algebraic expressions. By accumulating and equating to zero the power coefficients of the $\left(\frac{G'}{G^2}\right)$. The values of ρ_0, ρ_1, and σ_1 are derived by handling the resulting algebraic system.

Cluster 1:

$$\theta = 2\lambda\mu s^2\tau^2\alpha_2 + 8\mu\lambda s^2\tau^2\alpha_3 - \gamma^2\tau^2\alpha_2 - 4\gamma^2\tau^2\alpha_3 - \alpha_1 + 2\alpha_2 + 2\alpha_3,$$

$$\rho_0 = 0, \quad \rho_1 = \pm\sqrt{2}\tau s\lambda\sqrt{\frac{\alpha_2 + 4\alpha_3}{\alpha_4(y-1)}}, \quad \sigma_1 = 0.$$

Cluster 2:

$$\theta = -4\lambda\mu s^2\tau^2\alpha_2 - 16\mu\lambda s^2\tau^2\alpha_3 - \gamma^2\tau^2\alpha_2 - 4\gamma^2\tau^2\alpha_3 - \alpha_1 + 2\alpha_2 + 2\alpha_3,$$

$$\rho_0 = 0,$$

$$\rho_1 = \pm\tau s\lambda\sqrt{2}\sqrt{\frac{\alpha_2 + 4\alpha_3}{\alpha_4(y-1)}},$$

$$\sigma_1 = \pm\tau s\mu\sqrt{2}\sqrt{\frac{\alpha_2 + 4\alpha_3}{\alpha_4(y-1)}}.$$

Cluster 3:

$$\theta = 2\lambda\mu s^2\tau^2\alpha_2 + 8\mu\lambda s^2\tau^2\alpha_3 - \gamma^2\tau^2\alpha_2 - 4\gamma^2\tau^2\alpha_3 - \alpha_1 + 2\alpha_2 + 2\alpha_3,$$

$$\rho_0 = 0, \quad \rho_1 = 0, \quad \sigma_1 = \pm\tau s\mu\sqrt{2}\sqrt{\frac{\alpha_2 + 4\alpha_3}{\alpha_4(y-1)}}.$$

For **Cluster 1,** the subsequent solutions are built.

Case-1: If $\mu\lambda > 0$, then by using the Eq. (3), a family of trigonometric solution is presented as follows:

$$\Xi_{1,1}^{\pm}(x,t) = \left\{\frac{\sqrt{2}\tau s\lambda\sqrt{\frac{\alpha_2+4\alpha_3}{\alpha_4(y-1)}}\sqrt{\frac{\mu}{\lambda}}\begin{pmatrix}\Theta_1\cos\left(\sqrt{\mu\lambda}(sx-\eta t)\right) \\ +\Theta_2\sin\left(\sqrt{\mu\lambda}(sx-\eta t)\right)\end{pmatrix}}{\left(\Theta_2\cos\left(\sqrt{\mu\lambda}(sx-\eta t)\right) - \Theta_1\sin\left(\sqrt{\mu\lambda}(sx-\eta t)\right)\right)}\right\} \times \exp(i \times \{\gamma x + \theta t + \delta\}), \tag{48}$$

in which $\theta = 2\lambda\mu s^2\tau^2\alpha_2 + 8\mu\lambda s^2\tau^2\alpha_3 - \gamma^2\tau^2\alpha_2 - 4\gamma^2\tau^2\alpha_3 - \alpha_1 + 2\alpha_2 + 2\alpha_3$, and $\eta = 2\gamma s\tau^2(\alpha_2 + 4\alpha_3)$.

Case-2: If $\mu\lambda < 0$, then by using the Eq. (3), family of hyperbolic solution is given as follows:

$$\Xi_{1,2}^{\mp}(x,t) = \left\{\frac{\sqrt{2}\tau s\lambda\sqrt{\frac{\alpha_2+4\alpha_3}{\alpha_4(y-1)}}\sqrt{-\frac{\mu}{\lambda}}\begin{pmatrix}\Theta_1\cosh\left(2\sqrt{-\mu\lambda}(sx-\eta t)\right) \\ +\Theta_1\sinh\left(2\sqrt{-\mu\lambda}(sx-\eta t)\right)+\Theta_2\end{pmatrix}}{\left(\Theta_1\cosh\left(2\sqrt{-\mu\lambda}(sx-\eta t)\right) + \Theta_1\sinh\left(2\sqrt{-\mu\lambda}(sx-\eta t)\right) - \Theta_2\right)}\right\} \times \exp(i \times \{\gamma x + \theta t + \delta\}), \tag{49}$$

in which $\theta = 2\lambda\mu s^2\tau^2\alpha_2 + 8\mu\lambda s^2\tau^2\alpha_3 - \gamma^2\tau^2\alpha_2 - 4\gamma^2\tau^2\alpha_3 - \alpha_1 + 2\alpha_2 + 2\alpha_3$, and $\eta = 2\gamma s\tau^2(\alpha_2 + 4\alpha_3)$.

Case-3: If $\mu = 0,\ \lambda \neq 0$, then by using the Eq. (3), family of rational solution is noted as follows:

$$\Xi_{1,3}^{\mp}(x,t) = \left\{ \frac{\tau s\sqrt{2}\sqrt{\frac{\alpha_2+4\alpha_3}{\alpha_4(y-1)}}\Theta_1}{(\Theta_1(sx-\eta t)+\Theta_2)} \right\} \times \exp(i \times \{\gamma x + \theta t + \delta\}), \tag{50}$$

in which $\theta = 2\lambda\mu s^2\tau^2\alpha_2 + 8\mu\lambda s^2\tau^2\alpha_3 - \gamma^2\tau^2\alpha_2 - 4\gamma^2\tau^2\alpha_3 - \alpha_1 + 2\alpha_2 + 2\alpha_3$, and $\eta = 2\gamma s\tau^2(\alpha_2 + 4\alpha_3)$.

For **Cluster 2,** the subsequent solutions are built.

Case-1: If $\mu\lambda > 0$, then by using the Eq. (3), family of trigonometric solution is delivered as follows:

$$\Xi_{2,1}^{\mp}(x,t) = \left\{ \frac{\sqrt{2}\tau s\mu\sqrt{\frac{\alpha_2+4\alpha_3}{\alpha_4(y-1)}}(\Theta_1+\Theta_2)^2}{\sqrt{\frac{\mu}{\lambda}}\left(\Theta_1\sin\left(\sqrt{\mu\lambda}(sx-\eta t)\right)-\Theta_2\cos\left(\sqrt{\mu\lambda}(sx-\eta t)\right)\right) \times \left(\Theta_1\cos\left(\sqrt{\mu\lambda}(sx-\eta t)\right)+\Theta_2\sin\left(\sqrt{\mu\lambda}(sx-\eta t)\right)\right)} \right\} \times \exp(i \times \{\gamma x + \theta t + \delta\}), \tag{51}$$

in which $\theta = -4\lambda\mu s^2\tau^2\alpha_2 - 16\mu\lambda s^2\tau^2\alpha_3 - \gamma^2\tau^2\alpha_2 - 4\gamma^2\tau^2\alpha_3 - \alpha_1 + 2\alpha_2 + 2\alpha_3$, and $\eta = 2\gamma s\tau^2(\alpha_2 + 4\alpha_3)$.

Case-2: If $\mu\lambda < 0$, then by using the Eq. (3), family of hyperbolic solution is offered as follows:

$$\Xi_{2,2}^{\pm}(x,t) = \left\{ \frac{4\sqrt{2}\tau s\mu\Theta_1\Theta_2\sqrt{\frac{\alpha_2+4\alpha_3}{\alpha_4(y-1)}}\begin{pmatrix}\cosh\left(2\sqrt{-\mu\lambda}(sx-\eta t)\right)\\ +\sinh\left(2\sqrt{-\mu\lambda}(sx-\eta t)\right)\end{pmatrix}}{\sqrt{-\frac{\mu}{\lambda}}\begin{pmatrix}\Theta_1\cosh\left(2\sqrt{-\mu\lambda}(sx-\eta t)\right)\\ +\Theta_1\sinh\left(2\sqrt{-\mu\lambda}(sx-\eta t)\right)-\Theta_2\end{pmatrix} \times \begin{pmatrix}\Theta_1\cosh\left(2\sqrt{-\mu\lambda}(sx-\eta t)\right)\\ +\Theta_1\sinh\left(2\sqrt{-\mu\lambda}(sx-\eta t)\right)+\Theta_2\end{pmatrix}} \right\} \times \exp(i \times \{\gamma x + \theta t + \delta\}), \tag{52}$$

in which $\theta = -4\lambda\mu s^2\tau^2\alpha_2 - 16\mu\lambda s^2\tau^2\alpha_3 - \gamma^2\tau^2\alpha_2 - 4\gamma^2\tau^2\alpha_3 - \alpha_1 + 2\alpha_2 + 2\alpha_3$, and $\eta = 2\gamma s\tau^2(\alpha_2 + 4\alpha_3)$.

Case-3: If $\mu = 0,\ \lambda \neq 0$, then by using the Eq. (3), family of rational solution is illustrated as follows:

$$\Xi_{2,3}^{\mp}(x,t) = \left\{ \frac{\sqrt{2}\tau s\sqrt{\frac{\alpha_2+4\alpha_3}{\alpha_4(y-1)}}\begin{pmatrix}\Theta_1^2\lambda\mu(sx-\eta t)^2\\ +2\Theta_1\Theta_2\lambda\mu(sx-\eta t)\\ +\Theta_2^2\lambda\mu+\Theta_1^2\end{pmatrix}}{(\Theta_1(sx-\eta t)+\Theta_2)\Theta_1} \right\} \times \exp(i \times \{\gamma x + \theta t + \delta\}), \tag{53}$$

in which $\theta = -4\lambda\mu s^2\tau^2\alpha_2 - 16\mu\lambda s^2\tau^2\alpha_3 - \gamma^2\tau^2\alpha_2 - 4\gamma^2\tau^2\alpha_3 - \alpha_1 + 2\alpha_2 + 2\alpha_3$.

For **Cluster 3,** the subsequent solutions are built.

Case-1: If $\mu\lambda > 0$, then by using the Eq. (3), family of trigonometric solution is demonstrated as follows:

$$\Xi_{3,1}^{\pm}(x,t) = \left\{ \frac{\tau s\mu\sqrt{2}\sqrt{\frac{\alpha_2+4\alpha_3}{\alpha_4(y-1)}}\left(\Theta_2\cos\left(\sqrt{\mu\lambda}(sx-\eta t)\right)-\Theta_1\sin\left(\sqrt{\mu\lambda}(sx-\eta t)\right)\right)}{\sqrt{\frac{\mu}{\lambda}}\left(\Theta_1\cos\left(\sqrt{\mu\lambda}(sx-\eta t)\right)+\Theta_2\sin\left(\sqrt{\mu\lambda}(sx-\eta t)\right)\right)} \right\} \times \exp(i \times \{\gamma x + \theta t + \delta\}), \tag{54}$$

in which $\theta = 2\lambda\mu s^2\tau^2\alpha_2 + 8\mu\lambda s^2\tau^2\alpha_3 - \gamma^2\tau^2\alpha_2 - 4\gamma^2\tau^2\alpha_3 - \alpha_1 + 2\alpha_2 + 2\alpha_3$, and $\eta = 2\gamma s\tau^2(\alpha_2 + 4\alpha_3)$.

Case-2: If $\mu\lambda < 0$, then by using the Eq. (3), family of hyperbolic solution is shown as follows:

$$\Xi_{3,2}^{\mp}(x,t) = \left\{ \frac{\tau s\mu\sqrt{2}\sqrt{\frac{\alpha_2+4\alpha_3}{\alpha_4(y-1)}}\begin{pmatrix} \Theta_1 \cosh\left(2\sqrt{-\mu\lambda}\,(sx-\eta t)\right) \\ +\Theta_1 \sinh\left(2\sqrt{-\mu\lambda}\,(sx-\eta t)\right) - \Theta_2 \end{pmatrix}}{\sqrt{-\frac{\mu}{\lambda}}\begin{pmatrix} \Theta_1 \cosh\left(2\sqrt{-\mu\lambda}\,(sx-\eta t)\right) \\ +\Theta_1 \sinh\left(2\sqrt{-\mu\lambda}\,(sx-\eta t)\right) + \Theta_2 \end{pmatrix}} \right\} \times \exp(i \times \{\gamma x + \theta t + \delta\}), \tag{55}$$

in which $\theta = 2\lambda\mu s^2\tau^2\alpha_2 + 8\mu\lambda s^2\tau^2\alpha_3 - \gamma^2\tau^2\alpha_2 - 4\gamma^2\tau^2\alpha_3 - \alpha_1 + 2\alpha_2 + 2\alpha_3$, and $\eta = 2\gamma s\tau^2(\alpha_2 + 4\alpha_3)$.

Case-3: If $\mu = 0$, $\lambda \neq 0$, then by using the Eq. (3), family of rational solution is portrayed as follows:

$$\Xi_{3,3}^{\mp}(x,t) = \left\{ \frac{\tau s\lambda\mu\sqrt{2}\sqrt{\frac{\alpha_2+4\alpha_3}{\alpha_4(y-1)}}\left(\Theta_1(sx-\eta t)+\Theta_2\right)}{\Theta_1} \right\} \times \exp(i \times \{\gamma x + \theta t + \delta\}), \tag{56}$$

in which $\theta = 2\lambda\mu s^2\tau^2\alpha_2 + 8\mu\lambda s^2\tau^2\alpha_3 - \gamma^2\tau^2\alpha_2 - 4\gamma^2\tau^2\alpha_3 - \alpha_1 + 2\alpha_2 + 2\alpha_3$, and $\eta = 2\gamma s\tau^2(\alpha_2 + 4\alpha_3)$.

4 Modulation instability analysis

The interaction of nonlinear and dispersive processes causes modulation instability in steady states in a lot of nonlinear systems. Modulation instability is a widely investigated phenomenon that is particular to optical fibers and important for fiber optic communication system design. Here, the Kerr effect produces nonlinearity by altering the fiber's refractive index according to light intensity. The optical signal travels through the fiber and is represented by the wave field. Modulation instability is the process by which tiny perturbations in nonlinear wave equations can increase exponentially to create new patterns or structures. This section focuses on seeking linear stability techniques to examine the equation's modulation instability (MI) [44].

Let us assume that the perturbed solution is given by:

$$\Xi(x,t) = \left(\sqrt{P} + v(x,t)\right)e^{iP\epsilon x}, \tag{57}$$

where P is the normalized optical power. If we use the Eq. (57) in the Eq. (1), we get

$$\tau^2(\alpha_2+\alpha_3)v_{xx} + 2i\tau^2P(\alpha_2+\alpha_3)\epsilon v_x + iv_t + (-\alpha_1 + 2\alpha_2 + \alpha_3)v = 0. \tag{58}$$

Assume that a solution to Eq. (58) is given by:

$$v(x,t) = \gamma_1 e^{i(\kappa x - \omega t)} + \gamma_2 e^{-i(\kappa x - \omega t)}. \tag{59}$$

Here, κ is the normalized wave number and ω denotes the frequency. By integrating Eq. (59) into Eq. (58), and isolating the coefficients of $e^{i(\kappa x - \omega t)}$ and $e^{-i(\kappa x - \omega t)}$ to solve the determinant of the coefficient matrix, we obtain the following dispersion relation:

$$2\left(\kappa(\alpha_2+\alpha_3)\left(P\epsilon - \frac{\kappa}{2}\right)\tau^2 + \frac{\alpha_3}{2} - \frac{\omega}{2} - \frac{\alpha_1}{2} + \alpha_2\right) - 2\left(\left(P\epsilon + \frac{\kappa}{2}\right)\kappa(\alpha_2+\alpha_3)\tau^2 - \frac{\alpha_3}{2} - \frac{\omega}{2} + \frac{\alpha_1}{2} - \alpha_2\right) = 0. \tag{60}$$

By analyzing dispersion relation Eq. (60) for κ, we can derive

$$\kappa = \pm\frac{\sqrt{-(\alpha_2+\alpha_3)(\alpha_1 - 2\alpha_2 - \alpha_3)}}{(\alpha_2+\alpha_3)\tau}.$$

The dispersion relation that results provides information on the stability of the steady state. Whereas an imaginary κ indicates instability and leads to exponentially increasing perturbations, a real κ component indicates that the steady state is resilient to small disturbances.

5 Graphical explanations

In this section, we provide convincing illustrations of the precise solutions to the zig-zag equation that are found using the nGERFM and the $\left(\frac{G'}{G^2}\right)$-expansion function approach. The zig-zag equation's parameters and intrinsic nonlinearities can affect the precise form and properties of soliton solutions, which is an important point to take into account. The findings demonstrate the novelty of our research, which has not been documented in other published studies. We use a variety of visualization methods, which include 3D, contour, and 2D plots, to deepen the understanding of these soliton solutions. The dynamics of the wave solutions represented by Figs. 1, 2, 3 and 4 illustrate various physical behaviors of the system under study, governed by distinct parameter values.

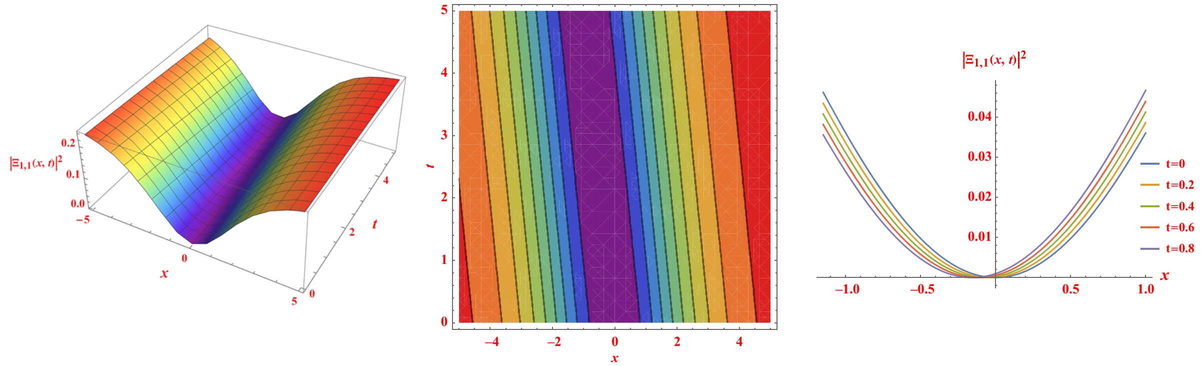

(a) (b) (c)

Fig. 1 The 3D, contour, and 2D plots for the $|\Xi_{1,1}(x,t)|^2$ in Eq. (18) by choosing the values $\alpha_1 = 2$, $\alpha_2 = 3$, $\alpha_3 = 1.7$, $\alpha_4 = 0.5$, $y = 2$, $s = 0.8$, $\gamma = -1$, $\tau = 0.1$, $\delta = 0$

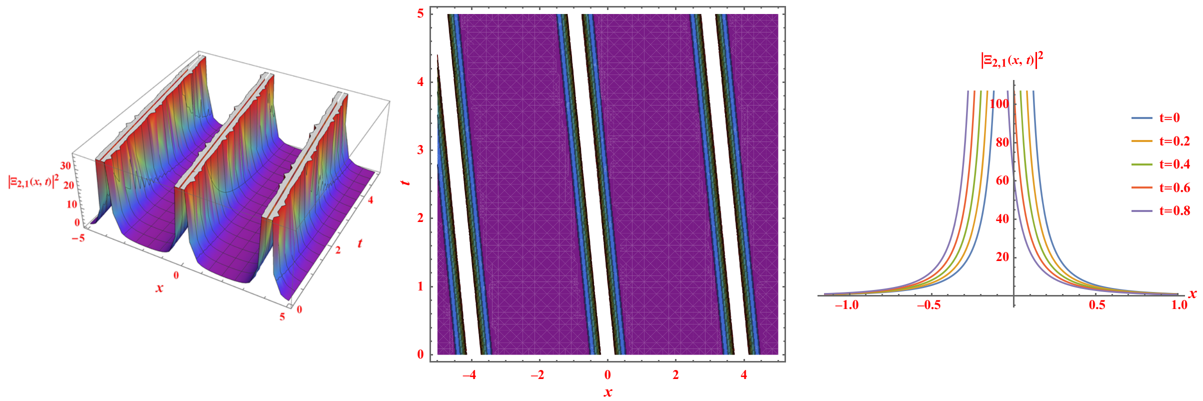

(a) (b) (c)

Fig. 2 The 3D, contour, and 2D plots for the $|\Xi_{2,1}(x,t)|^2$ in Eq. (23) by choosing the values $\alpha_1 = 0.7$, $\alpha_2 = 1.7$, $\alpha_3 = 0.7$, $\alpha_4 = 0.5$, $y = 5$, $s = 1.8$, $\gamma = 1.1$, $\tau = 0.5$, $\delta = 0$

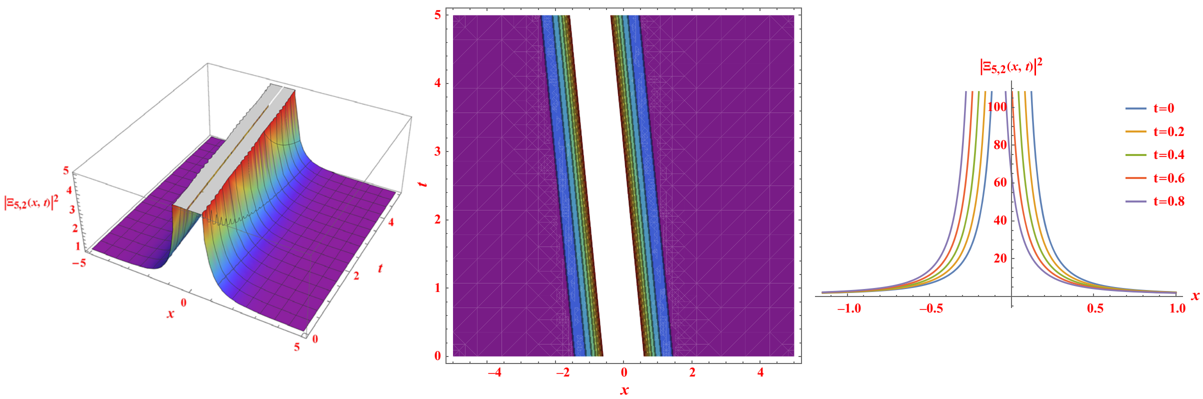

(a) (b) (c)

Fig. 3 The 3D, contour, and 2D plots for the $|\Xi_{5,2}(x,t)|^2$ in Eq. (38) by choosing the values $\alpha_1 = 2.2$, $\alpha_2 = 0.07$, $\alpha_3 = 3.2$, $\alpha_4 = 2.5$, $y = 5$, $s = 1.8$, $\gamma = 1.3$, $\tau = -0.5$, $\delta = 0$

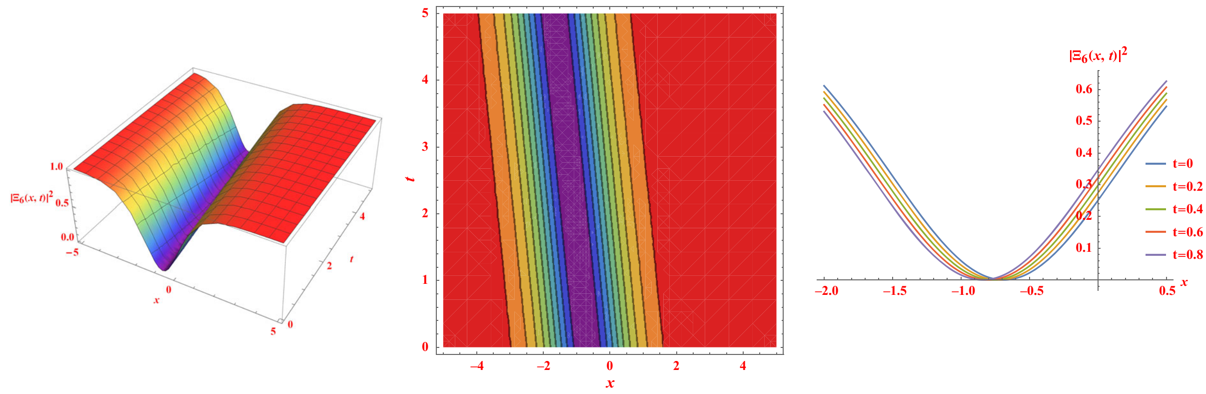

(a) (b) (c)

Fig. 4 The 3D, contour, and 2D plots for the $|\Xi_6(x,t)|^2$ in Eq. (43) by choosing the values $\alpha_1 = 0.7$, $\alpha_2 = 1.7$, $\alpha_3 = 0.2$, $\alpha_4 = 0.5$, $y = 5$, $s = 1.8$, $\gamma = 0.1$, $\tau = 1.5$, $\delta = 0$

Figure 1 depicts the 3D, contour, and 2D plots for $|\Xi_{1,1}(x,t)|^2$ derived from Eq. (18). The 3D plot reveals a localized structure with peaks and dips, characteristic of dark solitons, where the intensity decreases at specific points, demonstrating stable energy localization. The contour plot highlights the soliton's propagation path and intensity variations, while the 2D plot provides a temporal or spatial cross-section, showing oscillatory wave behavior. Figure 2 showcases $|\Xi_{2,1}(x,t)|^2$ from Eq. (23), where the lower parameter values lead to smoother waveforms with reduced steepness. The 3D representation captures the soliton's broader profile, while the contour plot emphasizes its periodic propagation, and the 2D plot reveals symmetric oscillations, indicative of system stability. Figure 3, corresponding to $|\Xi_{5,2}(x,t)|^2$ from Eq. (38), demonstrates sharper gradients and more complex waveforms due to higher parameter values, reflecting energetic or chaotic dynamics. The contour plot suggests irregular propagation patterns, potentially arising from instability, while the 2D plot reveals rapid oscillations and sensitive dependence on initial conditions. Finally, Fig. 4 illustrates $|\Xi_6(x,t)|^2$ from Eq. (43), depicting a smooth and extended wave structure. The 3D plot reveals a broader profile, suggesting weak nonlinearity and dominant dispersion. The contour plot highlights gradual intensity variations, indicating stable yet less localized energy distribution. The 2D plot further confirms smooth oscillatory behavior, reflecting minimal perturbations and a predictable wave evolution. Collectively, these findings demonstrate how variations in system parameters influence soliton stability, energy distribution, and potential chaotic behavior. In addition, the flexibility of these solutions to various parameter values allows the creation of a wide range of graphical visualizations, thereby enhancing our understanding of their behavior under different conditions.

6 Comparisons

In this part, we contrast our investigation's findings with those of earlier studies that used various analytical techniques and are reported in the literature. This comparative study aims to highlight the distinctive features and creative contributions of our current research. Riaz et al. obtained solutions for the studied equation using the generalized logistic equation method and the Sardar subequation approach [40]. They also analyzed the bifurcation theory and the chaotic behavior. Using two efficient methods, S. Kumar and A. Kumar developed for Eq. (1) a variety of soliton patterns [42]. By using semi-inverse techniques and collective variables to assess the investigated model, Alhussain and Raza achieved their goal of identifying bright solitons [43]. Our work synthesizes this research to apply a more effective technique, namely the nGERFM and the $\left(\frac{G'}{G^2}\right)$-expansion function approach. Thus, we provide new soliton solutions by combining these two approaches, including combo trigonometric, hyperbolic solutions in mixed form, exponential function, singular periodic, shock, trigonometric, hyperbolic, singular, and exponential solutions.

It is clear from the meticulous selection of the parameters used in the study that a large number of the findings are consistent with those of previous studies. Keep in mind that, despite possible similarities, these results were initially expressed differently from ours. A thorough search of relevant research was conducted, but no solution that was exactly the same as the one presented in this paper could be obtained. Our remaining results' novelty and ingenuity are highlighted by the fact that they do not appear to have been reported previously. Using both the nGERFM and the $\left(\frac{G'}{G^2}\right)$-expansion function approach, the results presented in this study were achieved.

7 Conclusion

In this study, a zig-zag optical lattice prototype for cold bosonic atoms was investigated using two analytical methods, namely the nGERFM and the $\left(\frac{G'}{G^2}\right)$-expansion function approach. To begin with, we regarded the nGERFM. The use of the nGERFM enabled us to obtain several classes of soliton solutions, including singular, shock, singular periodic, exponential, combo trigonometric, and hyperbolic solutions in mixed forms. Secondly, we considered the $\left(\frac{G'}{G^2}\right)$-expansion function approach. By using this method, we get trigonometric, hyperbolic, and rational soliton solutions. A key benefit of these techniques is their capability to predict and organize solution structures from the start. Mathematica was used to generate 3D, contour, and 2D plots. The soliton solutions found for the chosen parameter values were presented graphically. The logical and lucid methodology makes it possible for interested parties to solve their NLPDEs right away. According to the outcomes obtained, it is important to note that although the methods used in this paper contribute significantly to our understanding of soliton dynamics and their connection with the desired models, the offered methods fail when the largest derivative and the nonlinear terms are not homogeneously balanced. Despite these constraints, the present study demonstrates that the methods used in the paper are very effective, applicable, and beneficial for nonlinear models in different scientific areas. The modulation instability (MI) analysis performed on the model also contributes new insights. The soliton solutions we have achieved are original and unique to the zig-zag optical lattice prototype. Furthermore, in comparison to many previous studies, our discoveries offer a more exhaustive range of functions, including hyperbolic, rational, trigonometric, and exponential solutions. These validated new solutions are applicable for analyzing NLPDEs across fields such as applied sciences, quantum physics, plasma physics, mathematical physics, nonlinear dynamics, and engineering. In addition, the future aim of this study is to investigate the impact of the methods used in the area of specific models. The accuracy of each solution has been verified using the Maple software program.

Funding Open access funding provided by the Scientific and Technological Research Council of Türkiye (TÜBITAK).

Data availability This published article includes all data generated or analyzed during the trial.

Declarations

Conflict of interest The author reports that there is no conflict of interest.

References

1. Şenol, M.: Abundant solitary wave solutions to the new extended (3+1)-dimensional nonlinear evolution equation arising in fluid dynamics. Mod. Phys. Lett. B 2450475 (2024)
2. Muhammad, J., Rehman, S. U., Nasreen, N., Bilal, M., Younas, U.: Exploring the fractional effect to the optical wave propagation for the extended Kairat-II equation. Nonlinear Dyn. 1–12 (2024)
3. Liang, Y.H., Wang, K.J.: Bifurcation analysis, chaotic phenomena, variational principle, Hamiltonian, solitary and periodic wave solutions of the time-fractional Benjamin Ono equation. Fractals (2024)
4. Wang, K.J., Wang, G.D., Shi, F., Liu, X.L., Zhu, H.W.: Variational principle, Hamiltonian, bifurcation analysis, chaotic behaviors and the diverse solitary wave solutions of the sim-

plified modified Camassa-Holm equation. Int. J. Geometric Methods Mod, Phys (2024)
5. Wang, K.J., Liu, J.H.: Mathematical model and the solution of the capillary vibration in a nanoscale deformable. Math. Methods Appl, Sci (2025)
6. Wang, K.J., Li, S.: Novel complexiton solutions to the new extended (3+ 1)-dimensional Boiti-Leon-Manna-Pempinelli equation for incompressible fluid. Europhys, Lett (2024)
7. Wang, K.J., Wang, G.D., Shi, F.: Sub-picosecond pulses in single-mode optical fibres with the Kaup-Newell model via two innovative methods. Pramana **98**(1), 26 (2024)
8. Rafiq, M.N., Chen, H.: Multiple interaction solutions, parameter analysis, chaotic phenomena and modulation instability for a (3+ 1)-dimensional Kudryashov-Sinelshchikov equation in ideal liquid with gas bubbles. Nonlinear Dyn. 1–24 (2024)
9. Rafiq, M.N., Chen, H., Rafiq, M.H.: Stability analysis and multi-wave structures of the ill-posed Boussinesq equation arising in nonlinear physical science. Opt. Quant. Electron. **55**(14), 1243 (2023)
10. Rafiq, M.N., Chen, H.: Modulation instability, N-solitons, resonant multi-wave structures and other diverse interaction phenomena to the (2+ 1)-dimensional Kadomtsev-Petviashvili-Benjamin-Bona-Mahony equation. Qual. Theory Dyn. Syst. **24**(1), 13 (2025)
11. ur Rahman, M., Sun, M., Boulaaras, S., Baleanu, D.: Bifurcations, chaotic behavior, sensitivity analysis, and various soliton solutions for the extended nonlinear Schrödinger equation. Bound. Value Probl. **2024**(1), 15 (2024)
12. Younas, U., Yao, F., Nasreen, N., Khan, A., Abdeljawad, T.: On the dynamics of soliton solutions for the nonlinear fractional dynamical system: application in ultrasound imaging. Results Phys. **57**, 107349 (2024)
13. Ahmad, J., Mustafa, Z.: Multi soliton solutions and their wave propagation insights to the nonlinear Schrödinger equation via two expansion methods. In: Mathematics and Foundations, Quantum Studies, pp. 1–17 (2024)
14. Wang, K.J., Shi, F., Li, S., Xu, P.: Dynamics of resonant soliton, novel hybrid interaction, complex N-soliton and the abundant wave solutions to the (2+ 1)-dimensional Boussinesq equation. Alex. Eng. J. **105**, 485–495 (2024)
15. Wang, K.J.: The generalized (3+1)-dimensional B-type Kadomtsev-Petviashvili equation: resonant multiple soliton, N-soliton, soliton molecules and the interaction solutions. Nonlinear Dyn. **112**(9), 7309–7324 (2024)
16. Wang, K.J.: Multi-wave complexiton, multi-wave, interaction-wave and the travelling wave solutions to the (2+1)-dimensional Boiti-Leon-Manna-Pempinelli equation for the incompressible fluid. Pramana **98**(2), 47 (2024)
17. Alizadeh, F., Hosseini, K., Sirisubtawee, S., Hincal, E.: Classical and nonclassical Lie symmetries, bifurcation analysis, and Jacobi elliptic function solutions to a 3D-modified nonlinear wave equation in liquid involving gas bubbles. Bound. Value Probl. **2024**(1), 111 (2024)
18. Ma, W., Bilige, S.: Novel interaction solutions to the (3+ 1)-dimensional Hirota bilinear equation by bilinear neural network method. Mod. Phys. Lett. B 2450240 (2024)
19. Jhangeer, A., Raza, N., Ejaz, A., Rafiq, M.H., Baleanu, D.: Qualitative behavior and variant soliton profiles of the generalized P-type equation with its sensitivity visualization. Alex. Eng. J. **104**, 292–305 (2024)
20. Rafiq, M.N., Rafiq, M.H., Alsaud, H.: Chaotic response, multistability and new wave structures for the generalized coupled Whitham-Broer-Kaup-Boussinesq-Kupershmidt system with a novel methodology. Chaos Solitons Fractals **190**, 115755 (2025)
21. Khan, M.I., Farooq, A., Nisar, K.S., Shah, N.A.: Unveiling new exact solutions of the unstable nonlinear Schrödinger equation using the improved modified Sardar sub-equation method. Results Phys. **59**, 107593 (2024)
22. Muhammad, J., Riaz, M.B., Younas, U., Nasreen, N., Jhangeer, A., Lu, D.: Extraction of optical wave structures to the coupled fractional system in magneto-optic waveguides. Arab J. Basic Appl. Sci. **31**(1), 242–254 (2024)
23. Younas, U., Muhammad, J., Ismael, H.F., Murad, M.A.S., Sulaiman, T.A.: Optical fractional solitonic structures to decoupled nonlinear Schrödinger equation arising in dual-core optical fibers. Mod. Phys. Lett. B **39**(01), 2450378 (2025)
24. Tariq, K.U., Liu, J.G., Nisar, S.: New traveling-wave solutions for a nonlinear Dodd-Bullough-Mikhailov equation. Math. Methods Appl, Sci (2024)
25. Eslami, M., Ur Rehman, H., Iqbal, I., Jedi Abduridha, S.A., Mirzazadeh, M., Hashemi, M.S.: Extended hyperbolic function method for the model having cubic-quintic-septimal nonlinearity in weak nonlocal. Comput. Methods Differ, Equ (2024)
26. Kapoor, M.: A robust regime via Sumudu HPM for Schrödinger equation in different dimensions. Results Opt. **14**, 100619 (2024)
27. Veeresha, P., Akinyemi, L., Oluwasegun, K., Şenol, M., Oduro, B.: Numerical surfaces of fractional Zika virus model with diffusion effect of mosquito-borne and sexually transmitted disease. Math. Methods Appl. Sci. **45**(5), 2994–3013 (2022)
28. Kopçasız, B., Yaşar, E.: Adaptation of Caputo residual power series scheme in solving nonlinear time fractional Schrödinger equations. Optik **289**, 171254 (2023)
29. Sağlam, F.N.K., Kopçasız, B., Tariq, K.U.: Optical solitons and dynamical structures for the zig-zag optical lattices in quantum physics. Int. J. Theor. Phys. **64**(2), 1–20 (2025). https://doi.org/10.1007/s10773-025-05902-0
30. Muhammad, J., Younas, U., Almutairi, D.K., Khan, A., Abdeljawad, T.: Optical wave features and sensitivity analysis of a coupled fractional integrable system. Results Phys. **68**, 108060 (2025)
31. Muhammad, J., Younas, U., Khan, A., Abdeljawad, T., Almutairi, D.K.: On the study of double dispersive equation in the Murnaghan's rod: dynamics of diversity wave structures. Partial Differ. Equ. Appl. Math. **12**, 100916 (2024)
32. Muhammad, J., Younas, U., Rezazadeh, H., Hosseinzadeh, M.A., Salahshour, S.: On the investigation of fractional coupled nonlinear integrable dynamical system: dynamics of soliton solutions. Mod. Phys. Lett. B **38**(36), 2450380 (2024)
33. Younas, U., Hussain, E., Muhammad, J., Garayev, M., El-Meligy, M.: Bifurcation analysis, chaotic behavior, sensitivity demonstration and dynamics of fractional solitary waves to nonlinear dynamical system. Ain Shams Eng. J. **16**(1), 103242 (2025)

34. Raza, N., Rafiq, M.H., Alrebdi, T.A., Abdel-Aty, A.H.: New solitary waves, bifurcation and chaotic patterns of Coupled Nonlinear Schrodinger System arising in fibre optics. Opt. Quant. Electron. **55**(10), 853 (2023)
35. Rafiq, M.H., Jannat, N., Rafiq, M.N.: Sensitivity analysis and analytical study of the three-component coupled NLS-type equations in fiber optics. Opt. Quant. Electron. **55**(7), 637 (2023)
36. Rafiq, M.H., Riaz, M.B., Basendwah, G.A., Raza, N., Rafiq, M.N.: Dynamics of quasi-periodic, bifurcation, sensitivity and three-wave solutions for (n+ 1)-dimensional generalized Kadomtsev-Petviashvili equation. PLoS ONE **19**(8), e0305094 (2024)
37. Raza, N., Rafiq, M.H., Kaplan, M., Kumar, S., Chu, Y.M.: The unified method for abundant soliton solutions of local time fractional nonlinear evolution equations. Results Phys. **22**, 103979 (2021)
38. Alrebdi, H.I., Rafiq, M.H., Fatima, N., Raza, N., Rafiq, M.N., Alshahrani, B., Abdel-Aty, A.H.: Soliton structures and dynamical behaviors for the integrable system of Drinfel'd-Sokolov-Wilson equations in dispersive media. Results Phys. **46**, 106269 (2023)
39. Baldelli, N., Cabrera, C.R., Julià-Farré, S., Aidelsburger, M., Barbiero, L.: Frustrated extended Bose-Hubbard model and deconfined quantum critical points with optical lattices at the antimagic wavelength. Phys. Rev. Lett. **132**(15), 153401 (2024)
40. Riaz, M.B., Jhangeer, A., Kazmi, S.S. (2024). Optical soliton stability in zig-zag optical lattices: comparative analysis through two analytical techniques and phase portraits. Nonlinear Dyn. 1–23
41. Chang, X., Xie, J., Wu, T., Tang, B.: Modulational instability and quantum discrete breather states of cold bosonic atoms in a zig-zag optical lattice. Int. J. Theor. Phys. **57**, 2218–2232 (2018)
42. Kumar, S., Kumar, A.: Dynamical behaviors and abundant optical soliton solutions of the cold bosonic atoms in a zig-zag optical lattice model using two integral schemes. Math. Comput. Simul. **201**, 254–274 (2022)
43. Alhussain, Z.A., Raza, N.: New optical solitons with variational principle and collective variable strategy for cold bosons in zig-zag optical lattices. J. Math. **2022**(1), 3229701 (2022)
44. Kopçasız, B., Sağlam, Nur Kaya, F.: Exploration of soliton solutions for the Kaup-Newell model using two integration schemes in mathematical physics. Math. Methods Appl. Sci. (2025). https://doi.org/10.1002/mma.10684